Energy Economics 62 (2017) 139–154

Contents lists available at ScienceDirect

Energy Economics

journal homepage: www.elsevier.com/locate/eneco

Joint price and volumetric risk in wind power trading: A copula approach

A. Pircalabu[a,b,*], T. Hvolby[a], J. Jung[b], E. Høg[a]

[a] Department of Mathematical Sciences, Fredrik Bajers Vej 7G, 9220 Aalborg Øst, Denmark
[b] Neas Energy A/S, Skelagervej 1, 9000 Aalborg, Denmark

ARTICLE INFO

Article history:
Received 23 February 2016
Received in revised form 18 November 2016
Accepted 20 November 2016
Available online 9 December 2016

JEL classification:
C22
C51
C52
G13

Keywords:
Volumetric risk
Spot electricity price
Wind power production
Time-varying copula model
Risk management
Correlation risk

ABSTRACT

This paper examines the dependence between wind power production and electricity prices and discusses its implications for the pricing and the risk distributions associated with contracts that are exposed to joint price and volumetric risk. We propose a copula model for the joint behavior of prices and wind power production, which is estimated to data from the Danish power market. We find that the marginal behavior of the individual variables is best described by ARMA–GARCH models with non-Gaussian error distributions, and the preferred copula model is a time-varying Gaussian copula. As an application of our joint model, we consider the case of an energy trading company entering into longer-term agreements with wind power producers, where the fluctuating future wind power production is bought at a predetermined fixed price. We find that assuming independence between prices and wind power production leads to an underestimation of risk, as the profit distribution becomes left-skewed when the negative dependence that we find in the data is accounted for. By performing a simple static hedge in the forward market, we show that the risk can be significantly reduced. Furthermore, an out-of-sample study shows that the choice of copula influences the price of correlation risk, and that time-varying copulas are superior to the constant ones when comparing actual profits generated with different models.

© 2016 Elsevier B.V. All rights reserved.

1. Introduction

Since the European electricity market reforms in the late 1990's, the electricity markets have undergone considerable structural changes. Liberalization has led to extremely volatile electricity prices, and the prioritization of renewable energy sources in order to reduce CO_2 emissions has introduced further challenges in terms of financial risk management. One particular challenge that we study in this paper is related to the production uncertainty associated with wind power generation. Wind power is highly non-dispatchable and therefore fundamentally different from the more traditional thermal power sources in the sense that the production cannot be planned and controlled to the same extent. The dependency on weather variations (wind speed and air density among others) makes the exact future production of a wind turbine or wind-farm very hard to predict. Thus, in addition to facing price volatility, wind power generators are exposed to production uncertainty, often referred to as volumetric risk.

The joint exposure to price and volumetric risk can be further amplified by a high penetration ratio of wind power in the grid. This is due to the mechanism of day-ahead price formation, which is based on finding the equilibrium between supply and demand bids made to the exchange, where the supply curve is built according to merit order stack[1]. Because wind power has a very low marginal cost, a high production for a given hour will, other things being equal, pull the market clearing price downwards. Similarly, if wind power production is low for a given hour, demand will have to be met by either import or turning on more costly generating plants. The latter (and possibly the former) will, again other things being equal, pull the prices upward. This leads to prices and wind power production being negatively correlated, which depending on the strength of this correlation, enhances the joint price and volumetric risk significantly. Empirical evidence regarding this relation between spot electricity prices and wind power production has been demonstrated in the literature, e.g. Jónnson et al. (2010) for the Danish power market,

* Corresponding author.
E-mail addresses: anca@math.aau.dk (A. Pircalabu), thomas@math.aau.dk (T. Hvolby), jju@neasenergy.com (J. Jung), esben@math.aau.dk (E. Høg).

[1] Supply bids from different power stations are ranked according to their production costs, and the market clearing price corresponds to the highest bid needed to match demand.

http://dx.doi.org/10.1016/j.eneco.2016.11.023
0140-9883/© 2016 Elsevier B.V. All rights reserved.

Gelabert et al. (2011) for Spain, and Elberg and Hagspiel (2015) and Paraschiv et al. (2014) for Germany.

In practice, it is usually energy trading companies that act on the exchange on behalf of the producers. Due to increasing wind power production in some power markets, some trading companies offer, in addition to the management of production, a predetermined fixed price in exchange for the fluctuating production. Companies offering such insurances against price movements will naturally attempt to cover their exposure, and a typical solution that will eliminate some of the risk is to sell energy on the forward market corresponding to the expected wind power production. The remaining exposure will inevitably cause the energy trading companies to purchase energy on the spot market when being short, and dispose of excess energy on the spot market when expecting less than the realized production. Furthermore, the negative relationship between prices and wind power production adds an additional correlation risk: If being short, chances are that the missing energy will have to be bought at a higher price; similarly, if having to dispose of excess electricity, chances are that this will be sold at times of a lower price. As a result, the negative dependence between price and production introduces a “double” risk that is not straight forward to address or diminish without having a well-specified model for the dependence structure.

The problem of joint price and volumetric risk stems back some decades, and was first discussed in McKinnon (1967) in relation to the classical farmer's problem— who faces both price and production uncertainty at the time of harvest. In McKinnon (1967), the author considered futures as hedging instruments, and presented an explicit formula for the optimal position in futures contracts (from a minimum-variance perspective); this formula pointed out that the correlation between the two sources of uncertainty is an essential feature of the problem. Later, the work of Moschini and Lapan (1995) included options in the hedging portfolio due to the non-linearity of profit. More recently, energy related work on the subject became available, and some interesting discussions on the hedging of volumetric risk associated with consumers' load (demand-side risk) were presented in Oum and Oren (2009, 2010) and Coulon et al. (2013). In Oum and Oren (2009, 2010), the authors assumed bivariate lognormality for electricity prices and consumers' demand of electricity with a constant correlation, and focused on hedging strategies that 1) maximize the expected utility of the hedged profit and 2) maximize the expected profit subject to a Value-at-Risk constraint. In Coulon et al. (2013), the authors propose a structural model that captures the complex dependence structure of electricity price and load dynamics as a base for hedging. While many of the ideas in the existing literature regarding the hedging of volumetric risk can be used in our application, there are some major distinctions between supply-side volumetric risk (associated with wind power production) and demand-side volumetric risk (consumers' load) that pose some challenges when having to specify a joint model for day-ahead electricity prices and wind power production.

One issue of concern when considering a joint model for electricity prices and wind power production is that the price dynamics are very different from the production dynamics, causing us to expect the benchmark bivariate (log) normality assumption to be too restrictive;[2] in fact, the two variables might have univariate marginal distributions from different families, making it very challenging to decide upon a suitable bivariate density. The assumption of constant correlation might also prove too restrictive, and many studies have shown evidence of time-varying dependence between economic time series, see e.g. Avdulaj and Barunikl (2015), De Lira Salvatierra and Patton (2013), Dias and Embrechts (2004), Patton (2006), and Wen et al. (2012). Thus, before addressing issues such as the valuation of correlation risk in the context of fixed price obligations with fluctuating wind power production or the hedging of portfolios containing such obligations, a large part of this paper is concerned with developing a joint model that correctly characterizes the marginal behavior of electricity prices and wind power production and also their dependence structure. For this purpose, we propose the use of copula models.

Copulas are flexible tools that can be used to completely describe the dependence structure between random variables while allowing for arbitrary marginal distributions. They were introduced in the literature by Sklar (1959), and have found various applications in economics and finance over the past decades: See Cherubini and Luciano (2002) for the use of copulas in pricing different types of bivariate options, Embrechts et al. (1999) for an application to risk management, and Patton (2013) for a thorough review on copula-based models, including methods for estimation, inference and model-selection. Applications of copula models in energy markets are less common, but some examples are Alexander (2004), Benth and Kettler (2011), Elberg and Hagspiel (2015), and González-Pedraz et al. (2015).

Specifically, we offer two contributions: Firstly, we propose a flexible joint model that relaxes the assumption of bivariate normality and that accounts for the time variation we observe in the dependence structure. Our empirical study is based on data from the Danish power market; nonetheless, we expect our results to be generally applicable in all liberalized energy markets with a high penetration of wind power in the grid. By performing statistical tests and Monte Carlo simulation studies, we demonstrate that our proposed empirical model captures the joint distribution accurately, and also its time-varying behavior.

Secondly, we provide applications of our model that are of interest to e.g. an energy trading company managing a large share of wind turbines. We estimate the risk distribution and the price of correlation risk associated with a specific contract exposed to joint price and volumetric risk, i.e. a contract implying that an energy trading company offers wind power producers an insurance against price movements, by purchasing their fluctuating production at a predetermined fixed price. We show that the negative relation between prices and wind power production plays an important role both in relation to the pricing and the risk distribution of such contracts. We find that the price of correlation risk amounts to a significant percentage of the price of a regular fixed price agreement with no volumetric risk (a standard forward contract). Also, the risk distribution becomes left-skewed under the assumption of negative dependence compared to the case of independence. Lastly, we compare the out-of-sample performance of competing models, and show that time-varying copula models outperform the constant copula models.

This paper is organized as follows: Section 2 briefly introduces the notion of copula and the methodology used in building a joint model for electricity prices and wind power production. In Section 3, we apply the theory to data from the Danish power market. In Section 4, we present a simulation study and investigate how different wind scenarios affect the conditional distribution of spot electricity prices. Section 5 presents an application to pricing and risk management, and in Section 6 we conclude.

2. Modeling dependence with copula models

Formally, a d-dimensional copula is a distribution function $C(u_1, \ldots, u_d)$ defined on the unit cube $[0, 1]^d$ with uniform margins. Since our application is a bivariate one, we shall consider the case where $d = 2$, however copula theory holds for the general multivariate case. The central result when working with copula models is Sklar's theorem, which shows how to decompose a joint distribution function into its univariate marginal distribution functions and a copula.

[2] Alone the fact that electricity prices can go negative rules out the lognormality assumption in some marketplaces.

In our application, we wish to condition on the information generated by past observations of our variables, denoted by $\mathcal{F}_{t-1}$. Thus, we shall consider an extension to Sklar's theorem proposed in Patton (2006), which holds for conditional joint distributions. The theorem states that if we let $F(\cdot \mid \mathcal{F}_{t-1})$ be the bivariate conditional distribution function of the random vector $\boldsymbol{Y}_t \equiv (Y_{1,t}, Y_{2,t})'$, with conditional marginal distribution functions $F_1(\cdot \mid \mathcal{F}_{t-1})$ and $F_2(\cdot \mid \mathcal{F}_{t-1})$, then there exists a two dimensional conditional copula $C(\cdot \mid \mathcal{F}_{t-1})$, such that

$$F((y_1, y_2) \mid \mathcal{F}_{t-1}) = C(F_1(y_1 \mid \mathcal{F}_{t-1}), F_2(y_2 \mid \mathcal{F}_{t-1}) \mid \mathcal{F}_{t-1}). \tag{1}$$

Furthermore, if the marginal distribution functions are continuous, the copula is unique. The converse also holds, such that given two conditional marginal distributions, we can use the conditional copula to link the variables to form a conditional joint distribution with the specified margins. It is especially this second part of the theorem that is useful here, since it allows us to isolate the description of the dependence structure from the marginal behavior of the individual variables.

Moreover, let us define the probability integral transform variables

$$U_{i,t} \equiv F_i(Y_{i,t} \mid \mathcal{F}_{t-1}), \quad \text{for } i = 1, 2, \tag{2}$$

and let $\boldsymbol{U}_t \equiv (U_{1,t}, U_{2,t})'$. Then $U_{i,t} \sim \text{Unif}(0,1)$, and note furthermore that the conditional copula in Eq. (1) is simply the conditional distribution of $\boldsymbol{U}_t \mid \mathcal{F}_{t-1}$:

$$\boldsymbol{U}_t \mid \mathcal{F}_{t-1} \sim C(\cdot \mid \mathcal{F}_{t-1}). \tag{3}$$

In this paper, we consider different copulas from the elliptical and archimedean families, which are commonly used in the financial literature. For a detailed treatment of these copulas and their properties, we refer to the reference books by Joe (1997) and Nelsen (1999).

2.1. Marginal models

As a first step when working with copulas, we need to find proper marginal distribution models. Here, we restrict our attention to marginal models of the ARMA–GARCH type to model the conditional mean and the conditional variance of the individual variables.[3] For example, an ARMA(p,q)–GARCH(1, 1) model for the margins can be written as

$$Y_{i,t} = \sum_{j=1}^{p} \phi_{i,j} Y_{i,t-j} + \sum_{k=1}^{q} \theta_{i,k} \varepsilon_{i,t-k} + \varepsilon_{i,t}, \tag{4}$$

$$\varepsilon_{i,t} = \sigma_{i,t} \eta_{i,t}, \tag{5}$$

$$\sigma_{i,t}^2 = \omega_i + \alpha_i \varepsilon_{i,t-1}^2 + \beta_i \sigma_{i,t-1}^2, \tag{6}$$

for $i = 1, 2$, where ω_i, α_i, β_i follow the restrictions posed in e.g. Nelson and Cao (1992), and $\alpha_i + \beta_i < 1$. Furthermore,

$$\eta_{i,t} \mid \mathcal{F}_{t-1}^{(i)} \sim F_i(0,1), \quad \text{for} \quad i = 1, 2 \text{ and all } \quad t. \tag{7}$$

[3] A variety of other parametric specifications can be considered for the conditional mean, such as ARMAX models, long memory models, linear and non-linear regression models. The same holds for the conditional variance where, among others, different extensions to the ARCH model can be considered; see Bollerslev (2008) for a long list of such models.

For the marginal distributions we consider the case where F_i does not vary with time and has a parametric form. Also, we relax the normality assumption, allowing for more general distributions. The ARMA–GARCH models function as filters that produce innovation processes $\eta_{1,t}$ and $\eta_{2,t}$ that are serially independent; it is the conditional distributions of $\eta_{1,t}$ and $\eta_{2,t}$ that are then coupled using the conditional copula.

One note of caution has to be made regarding the conditioning set $\mathcal{F}_{t-1}$ emphasizing that this set is generated by $(\boldsymbol{Y}_{t-1}, \boldsymbol{Y}_{t-2}, \dots)$. In our specification for the marginal models however, we do not condition on $\mathcal{F}_{t-1}$, but only a subset $\mathcal{F}_{t-1}^{(i)} \subset \mathcal{F}_{t-1}$. When using such models, the copula is, according to Fermanian and Wegkamp (2012), a true copula if and only if

$$Y_{i,t} \mid \mathcal{F}_{t-1} \stackrel{d}{=} Y_{i,t} \mid \mathcal{F}_{t-1}^{(i)}, \tag{8}$$

for $i = 1, 2$ and all t. If the equality in Eq. (8) is not satisfied, then the joint conditional distribution of $\boldsymbol{Y}_t \mid \mathcal{F}_{t-1}$ does not have the specified conditional marginal distributions. To study if the equality in Eq. (8) holds, we test for cross-equation effects by including lags of one variable in the conditional mean equation of the other variable and vice versa, and perform a standard Wald test for the joint significance of the added explanatory variables, as proposed in Patton (2013).

2.2. Estimation procedure for the joint model

To estimate the joint model, we perform maximum likelihood estimation. The joint conditional density is obtained by differentiating the joint conditional distribution function in Eq. (1). Thus, the log-likelihood function takes the form

$$\begin{aligned}\log \mathcal{L} &= \sum_{t=1}^{T} \log f((y_{1,t}, y_{2,t}) \mid \mathcal{F}_{t-1}; \Theta) = \sum_{t=1}^{T} \log f_1(y_{1,t} \mid \mathcal{F}_{t-1}; \Theta_1) \\ &\quad + \sum_{t=1}^{T} \log f_2(y_{2,t} \mid \mathcal{F}_{t-1}; \Theta_2) + \sum_{t=1}^{T} \log c((u_{1,t}, u_{2,t}) \mid \mathcal{F}_{t-1}; \gamma),\end{aligned} \tag{9}$$

where f_1 and f_2 are the conditional marginal densities, c is the conditional copula density defined as

$$c((u_{1,t}, u_{2,t}) \mid \mathcal{F}_{t-1}) = \frac{\partial^2}{\partial u_1 \partial u_2} C((u_{1,t}, u_{2,t}) \mid \mathcal{F}_{t-1}), \tag{10}$$

and

$$u_{i,t} = F_i(y_{i,t} \mid \mathcal{F}_{t-1}; \Theta_i), \quad \text{for } i = 1, 2. \tag{11}$$

In Eq. (9), Θ denotes the set of parameters for the entire model, and Θ_1, Θ_2 and γ denote the parameters for the two marginal models and the copula, respectively, and have no common elements. For simplicity, we assume that the copula is completely described by one single parameter γ. We perform multi-stage maximum likelihood estimation, where we consider the two marginal models and the copula model separately. For details on the validity of this procedure, consult Patton (2013).

2.3. Time-varying copula models

Since the dependency between electricity prices and wind power production might change through time, extending copula models to allow for time-varying dependence is relevant. Before specifying a parametric model for the copula dependence parameter, it is useful to investigate what type of time variation (if any) we can detect in the data. Here, we employ two tests proposed in Patton (2013): One that tests for the presence of a break in the rank correlation by performing the classical "sup" test, and another that tests for the presence of autocorrelation in a measure of dependence. For a comprehensive description of the two tests the reader is referred to Patton (2013).

2.3.1. The Generalized Autoregressive Score model

To model time-varying dependence, we employ the *Generalized Autoregressive Score* (GAS) model of Creal et al. (2013). In order to ease the presentation, we consider the case where the copula has one dependence parameter. For the GAS(1,1) model, a possible updating equation for the transformed copula dependence parameter g_{t+1} is:

$$g_{t+1} = \omega + \alpha g_t + \beta I_t^{-\frac{1}{2}} s_t, \tag{12}$$

where

$$\begin{aligned} g_t &= h(\gamma_t), \\ s_t &= \frac{\partial}{\partial \gamma} \log c((u_{1,t}, u_{2,t}); \gamma_t), \\ I_t &= \mathbb{E}_{t-1}\left[s_t^2\right]. \end{aligned}$$

In Eq. (12), s_t denotes the score of the copula log-likelihood and I_t is the Fisher information. Moreover, γ_t denotes the time-varying copula dependence parameter, which is usually constrained to lie in a particular range; see Table A.9 in Appendix A for details regarding the range of different copula dependence parameters. For estimation purposes, we apply a transformation $h(\cdot)$ to γ_t, to obtain g_t which takes values on the entire real axis. We note that the updating mechanism given in Eq. (12) is one of many possible specifications: The GAS model can be extended to include e.g. more lags or exogenous variables. Moreover, the scaling quantity $I_t^{-1/2}$ is simply one convenient choice. GAS models can be generalized to allow for asymmetries or long memory, and to include regime-switching, however such extensions are not considered in the present work.

The parameter estimates from the GAS model can be obtained by maximum likelihood estimation, as proposed by Creal et al. (2013). The only challenge can be finding a closed-form expression for the Fisher information, and thus deriving the updating mechanism in Eq. (12). To overcome this issue, the Fisher information is evaluated numerically for most copula specifications by performing the following steps:

1. Given a copula specification, construct a grid of values for the dependence parameter, $\left[\gamma^{(1)} < \gamma^{(2)} < \cdots < \gamma^{(n)}\right]$.
2. For each dependence parameter in the grid,
   (a) perform a large number of simulations from the chosen copula model,
   (b) evaluate the score function at each simulation,
   (c) compute the Fisher information, by taking the mean over the evaluated scores squared.
3. Finally, use linear interpolation to get the Fisher information at intermediate points.

2.4. Quantile dependence

As a preliminary study before specifying copula models, one can examine the dependence in the data by considering quantile dependence. For the case of negatively dependent variables, the quantile dependence is defined as:

$$\lambda^q = \begin{cases} \mathbb{P}(U_{1,t} \le q \mid U_{2,t} \ge 1-q), & 0 < q \le 1/2, \\ \mathbb{P}(U_{1,t} > q \mid U_{2,t} < 1-q), & 1/2 < q < 1. \end{cases} \tag{13}$$

By computing quantile dependence coefficients at different quantiles q, we obtain a richer description of the dependence structure. This can help narrow down the set of possible parametric copulas to a collection of models that are able to capture some of the characteristics we observe in the data. To obtain standard errors for the quantile dependence coefficients, we use bootstrapping; specifically, we follow the procedure proposed in Patton (2013), which is based on the stationary block-bootstrap of Politis and Romano (1994), where the optimal block-length is chosen according to Politis and White (2004) and Politis et al. (2009).[4]

2.5. Selection of copula models

To test for whether or not a copula is well specified, we perform two widely used goodness-of-fit (GoF) tests: The Kolmogorov–Smirnov (KS) and the Cramer–von Mises (CvM) tests. Under the null that the conditional copula is well specified, we should find that the empirical copula provides a good nonparametric estimate of the null conditional copula. Suppose we have the random sample $\{\boldsymbol{u}_t\} = \{(u_{1,t}, u_{2,t})\}_{t=1}^T$ from $\boldsymbol{U}_t$. Then the test statistics can be written as

$$KS^{(C)} = \max_t \left| C(\boldsymbol{u}_t; \hat{\gamma}) - \hat{C}(\boldsymbol{u}_t) \right|, \tag{14}$$

$$CvM^{(C)} = \sum_{t=1}^{T} \left\{ C(\boldsymbol{u}_t; \hat{\gamma}) - \hat{C}(\boldsymbol{u}_t) \right\}^2, \tag{15}$$

where $C(\boldsymbol{u}_t; \hat{\gamma})$ is an estimator of the null conditional copula. Moreover, $\hat{C}$ denotes the empirical copula defined as

$$\hat{C}(\boldsymbol{z}) \equiv \frac{1}{T+1} \sum_{t=1}^{T} \boldsymbol{1}\{u_{1,t} \le z_1, u_{2,t} \le z_2\}, \tag{16}$$

where $\boldsymbol{1}$ denotes the indicator function and $\boldsymbol{z} = (z_1, z_2) \in [0,1]^2$. The KS and CvM tests described above work solely for the testing of constant copula models. A slight modification will however allow for the additional testing of time-varying copulas: The KS and CvM tests based on the Rosenblatt transform. In our case, the transformation is simply

$$V_{1,t} = U_{1,t} \tag{17}$$

$$V_{2,t} = C_{2|1,t}(U_{2,t} | U_{1,t}; \hat{\gamma}_t), \tag{18}$$

where $C_{2|1,t}$ denotes the conditional copula of the random variable $U_{2,t}|U_{1,t}$. Applying the Rosenblatt transform to the data will yield *iid* and Unif(0, 1) variables, and hence we can compare the empirical copula of a random sample $\{\boldsymbol{v}_t\} = \{(v_{1,t}, v_{2,t})\}_{t=1}^T$ from $\boldsymbol{V}_t$, against the independence copula, defined as

$$C^{indep}(\boldsymbol{v}_t; \hat{\gamma}_t) \equiv \prod_{i=1}^{2} v_{i,t}. \tag{19}$$

A simulation-based approach is used to obtain p-values for the GoF tests described above, since the test statistics in Eqs. (14) and (15) depend on estimated parameters. This approach is described in detail in Berg (2009), Genest et al. (2009) and Patton (2013), and will not be elaborated on here.

Another very important issue when dealing with copulas is choosing the best copula model among competing models. Here, we

[4] The same bootstrapping procedure can be used to perform inference on other measures of dependence, e.g. linear correlation, rank correlation.

consider pairwise comparisons, where we follow Rivers and Vuong (2002) for most in-sample (IS) model comparisons and Diks et al. (2010) for out-of-sample (OOS) model comparisons. The IS comparison test can be performed when the models are non-nested; for the case where the models are nested, a likelihood ratio test can usually be used. The OOS model comparison test works for both nested and non-nested models. Also, both tests can be applied regardless of whether the copula is constant or time-varying.

For the IS case, the idea is to compare two models using their joint log-likelihood, and test the null

$$H_0 : \mathbb{E}\left[\boldsymbol{L}^{(1)} - \boldsymbol{L}^{(2)}\right] = 0, \tag{20}$$

against

$$H_1 : \mathbb{E}\left[\boldsymbol{L}^{(1)} - \boldsymbol{L}^{(2)}\right] > 0 \quad \text{and} \quad H_2 : \mathbb{E}\left[\boldsymbol{L}^{(1)} - \boldsymbol{L}^{(2)}\right] < 0, \tag{21}$$

where the superscripts (1) and (2) denote two competing models. The case of comparing joint log-likelihoods reduces in our case to comparing copula log-likelihoods, c.f. Eq. (9), since we use the same marginal distribution models. Hence, $\boldsymbol{L}^{(i)} = \log c^{(i)}(\boldsymbol{u}; \gamma^{(i)})$ or $\boldsymbol{L}^{(i)} = \log c^{(i)}(\boldsymbol{u}; \gamma_t^{(i)})$, $i = 1, 2$, depending on whether the copula is constant or time-varying. Rivers and Vuong (2002) show that under the null,

$$\frac{\sqrt{T}\left(\bar{L}^{(1)} - \bar{L}^{(2)}\right)}{\sqrt{\hat{\sigma}^2}} \xrightarrow{d} \mathrm{N}(0, 1) \tag{22}$$

where

$$\bar{L}^{(i)} = \frac{1}{T}\sum_{t=1}^{T} \log c^{(i)}\left(\hat{\boldsymbol{u}}_t; \hat{\gamma}_t^{(i)}\right), \quad \text{for } i = 1, 2. \tag{23}$$

As an estimator for the asymptotic variance of $\sqrt{T}\left(\bar{L}^{(1)} - \bar{L}^{(2)}\right)$ we use the Newey–West heteroskedasticity and autocovariance consistent (HAC) estimator.

For OOS comparisons, we consider a fixed estimation window, where the model is estimated using the data from $[1, T]$. We then evaluate the conditional predictive ability of two competing copulas on the OOS period, i.e. on R observations, where $R = T^* - T$, $T^* > T$. The test for comparing the predictive ability of competing copula models conditional on the estimated parameters proposed by Diks et al. (2010) is in fact a special case of the more general framework presented in Giacomini and White (2006). The null hypothesis for the OOS case is the same as for the IS case, and a test statistic based on the difference between the sample averages of the copula log-likelihoods can again be used, and is shown by Giacomini and White (2006) to be asymptotically $\mathrm{N}(0, 1)$ under the null. As an estimator for the asymptotic variance, we use the HAC estimator.

3. Empirical results

A joint model for electricity prices and wind power production is interesting to consider in an area with a high penetration ratio of wind power in the grid. Here, we analyze data from Denmark, which has long been among the top wind power producing countries. According to *Energinet.dk*, the Danish Transmission System Operator, more than a third of the Danish power consumption was covered by wind power in 2013, and in December that year, 57.4% of the consumption came from wind turbines. In 2014, wind turbines produced on average what corresponds to over 39% of the Danish power consumption. Also, in January 2014, 61.7% of the consumption was covered by wind power.

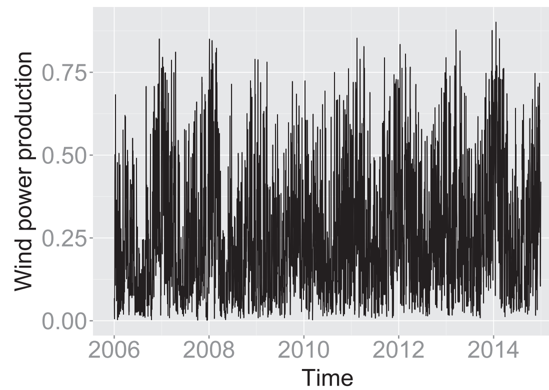

(a) Daily wind power production measured relative to the total installed capacity.

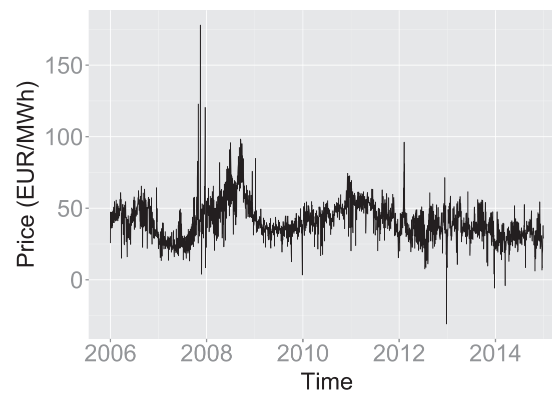

(b) Daily spot electricity prices

Fig. 1. Historical daily observations for the DK1 price area in the period 01/01/2006 to 31/12/2014.

Specifically, we base our analysis on data from one of the two Danish price areas, DK1 (Western Denmark), and a sample period that spans from 01/01/2006 to 31/12/2014. The first time series, Fig. 1 (a), consists of total daily wind power production in DK1 relative to the total installed capacity, and is obtained by performing the normalization

$$\frac{\text{Total daily wind power production (MWh)}}{\text{Installed capacity (MW)} \cdot H} \tag{24}$$

for each day in the sample, where H denotes the total number of hours in the day. We note that we work in UTC time, so $H = 24$ always. The second time series, Fig. 1 (b), represents the daily average of spot electricity prices.[5],[6]

Before proceeding to the estimation of a joint model for prices and wind power production, two comments are in order. First, since the production series is bounded, with a lower bound at 0 and an upper bound at 1, we perform a logistic transformation in order to obtain data that can take values on the entire real line. Second, we split our data into an in-sample (IS) period spanning from

[5] The data is publicly available on *Energinet.dk* and on the web page of Nord Pool's Elspot market, *nordpoolspot.com*. Elspot is a day-ahead physical delivery market for electricity currently operating in the Nordic and Baltic region.

[6] We note that one observation has been truncated in the price data, corresponding to the date 07/06/13, since this is assessed to be an outlier. On this date, the hourly price reached Nord Pool's cap price due to a combination of low wind, reduced import possibilities caused by planned maintenance on transmission cables and also planned maintenance on central power stations.

Table 1
The first panels display parameter estimates together with their std. errors in parenthesis. The last panel displays the results of GoF tests.

	Daily wind power production ARMA(1,3)–GARCH(1,1)	Daily spot electricity prices ARMA(3,1)–GARCH(1,1)
Conditional mean		
$\hat{\phi}_1$	0.8725 (0.0510)	1.4579 (0.0065)
$\hat{\phi}_2$	–	−0.5525 (0.0176)
$\hat{\phi}_3$	–	0.0897 (0.0261)
$\hat{\theta}_1$	−0.3578 (0.0550)	−0.8365 (0.0128)
$\hat{\theta}_2$	−0.2733 (0.0363)	–
$\hat{\theta}_3$	−0.0610 (0.0264)	–
Conditional variance		
$\hat{\omega}$	0.0803 (0.1269)	2.4433 (0.7388)
$\hat{\alpha}$	0.0251 (0.0199)	0.1657 (0.0312)
$\hat{\beta}$	0.9022 (0.1333)	0.7832 (0.0410)
Skewed general error dist./Skewed t dist.		
Shape $\hat{\nu}$	2.1348 (0.0967)	4.9967 (0.4711)
Skewness $\hat{\xi}$	0.8024 (0.0269)	0.9583 (0.0222)
Goodness-of-fit tests		
KS (p-val.)	0.6293	0.7097
CvM (p-val.)	0.5882	0.5996

01/01/2006 to 31/12/2012, and an out-of-sample (OOS) spanning from 01/01/2013 to 31/12/2014. Estimation of marginal models and copulas is performed on the IS data.

3.1. Marginal specifications for spot electricity prices and wind power production

Prior to modeling the dependence structure of electricity prices and wind power production, we filter out the stylized facts affecting the marginal behavior of the individual variables. As a first step, we demean and correct for deterministic seasonality by performing a regression on a constant and dummy variables. Specifically, we have used the dummy variable *month-of-year* to correct the (transformed) wind power production series for seasonality. For the price series both *day-of-week* and *month-of-year* dummy variables were used as regressors. To model the conditional mean and variance of the variables, we consider ARMA–GARCH models with different specifications for the error distribution. We consider ARMA models up to order (7,7), and GARCH models up to order (2,2). Based on the Bayesian Information Criterion, we find that the optimal model for the wind power production series is an ARMA(1,3)–GARCH(1,1), and use a skewed generalized error distribution for the standardized residuals. For the day-ahead electricity prices, we find the optimal model to be an ARMA(3,1)–GARCH(1,1), and use a skewed t distribution for the standardized residuals. Table 1 summarizes the estimation results, and Fig. B.10 in Appendix B displays the autocorrelation functions, histograms and quantile plots for the standardized residuals resulting from the fitted models. A visual inspection of Fig. B.10 shows that almost no autocorrelation is left in the standardized residuals. The specified distributions provide a reasonable fit, however we observe some deviations in the tails of both distributions. We complement these findings with GoF tests, where we consider the KS and CvM tests. The resulting p-values are given in Table 1 and indicate that there is not sufficient evidence as to reject the null that the distributional assumptions are well-specified.[7] We note that finding suitable marginal models is of great concern when working with copula models, since the copula takes as input *iid* Unif(0, 1) variables that result from applying the probability integral transform to the standardized residuals. A violation of the assumptions will thus automatically lead to a misspecified copula model.

Because we condition with different information sets when specifying the marginal models, we need to investigate whether or not lagged values of wind power production help explain electricity prices and vice versa. To do this, we consider the specified models for the conditional mean with added explanatory variables consisting of seven lagged values of the "other" series, and test for the significance of cross-sectional effects by performing a Wald test. For the wind power production, we consider an ARMAX(1,3,7) model, and for the electricity prices, we consider an ARMAX(3,1,7) model. The tests yield a p-value of 0.25 for the wind power production model, and 0.09 for the electricity price model, thus suggesting no cross-equation effects at a 5% significance level.[8]

Table 2
Estimated dependence measures with 95% confidence intervals based on the block-bootstrap procedure described in Section 2.4 and $M = 999$ bootstrap samples.

	Spearman's ρ	Kendall's τ	Linear correlation
Estimate	−0.5024	−0.3478	−0.5030
95% CI	(−0.5716, −0.4332)	(−0.3987, −0.2969)	(−0.5714, −0.4347)

3.2. Symmetric vs. asymmetric dependence

Having decided upon the marginal models for price and wind power production, the remaining of this section focuses on the modeling of the dependence structure. First, we apply the probability integral transform to the standardized residuals resulting from the marginal models to obtain approximately uniformly distributed variables. To perform this transformation, we use the estimated parametric models for the distribution functions F, i.e. the estimated skewed generalized error distribution and skewed t distribution, see Table 1. We obtain

$$\hat{U}_{W,t} = F_{skew\ \ ged}\left(\hat{\eta}_{W,t}, \hat{\nu}_W, \hat{\xi}_W\right) \tag{25}$$

$$\hat{U}_{S,t} = F_{skew\ \ t}\left(\hat{\eta}_{S,t}, \hat{\nu}_S, \hat{\xi}_S\right), \tag{26}$$

where $\hat{U}_{W,t}$ and $\hat{U}_{S,t}$ denote the resulting uniforms corresponding to the wind power production time series and the spot price time series, respectively. Standardized residuals are denoted by $\hat{\eta}$, and estimated distribution parameters are denoted by $\hat{\xi}$ (skew parameter) and $\hat{\nu}$ (shape parameter).

As an introductory investigation of the dependence structure, we compute some measures of dependence for $\hat{\boldsymbol{U}}_W$ and $\hat{\boldsymbol{U}}_S$. Table 2 displays the estimated coefficients for Spearman's ρ, Kendall's τ and linear correlation, implying (not surprisingly) that prices and wind power production are negatively correlated. Based on Eq. (13) we also compute quantile dependence measures, and the results, displayed in Fig. 2, show evidence for a symmetric dependence structure. When considering the farther right and left portions of Fig. 2 (a), the results reveal a slightly larger probability of observing low prices given that the production is high than the opposite. However, according to Fig. 2 (b), this difference is not statistically significant.

3.3. Constant copula models

Although we anticipate time-variation in the dependence structure, we consider six constant copula models, to have as benchmarks

[7] We perform simulation-based GoF tests, that take the parameter estimation errors from the ARMA–GARCH models into account. Specifically, we test for whether or not the probability integral transforms implied by the estimated conditional densities are *iid*Unif(0, 1). The p-values for the tests are based on 999 simulations.

[8] We have tried testing for cross-sectional effects with different other specifications, and none of the results indicate cross-equation effects at a 5% significance level.

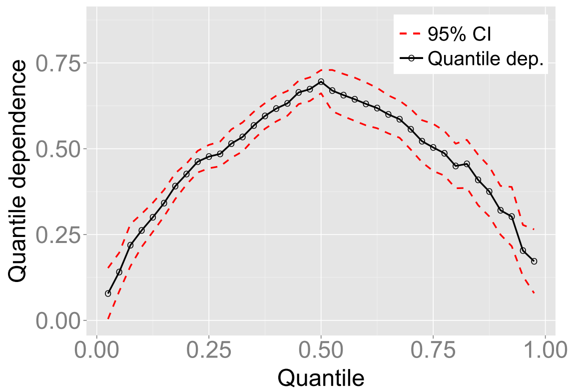

(a) Quantile dependence

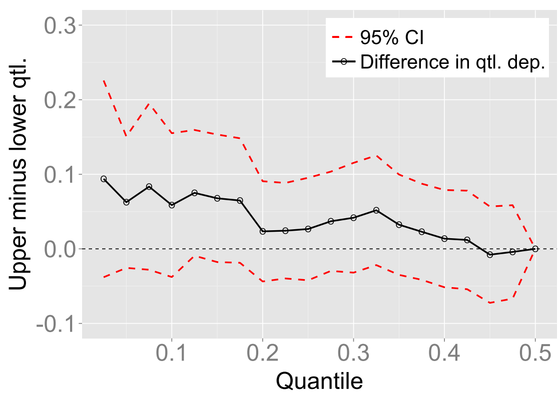

(b) Difference in quantile dependence

Fig. 2. Fig. 2 (a) displays estimated quantile dependence for quantile $q \in [0.025, 0.975]$ and a size step of 0.025, along with a 95% confidence interval based on the block-bootstrap procedure described in Section 2.4 and $M = 999$ bootstrap samples. The y-axis provides the probability of $\hat{\boldsymbol{U}}_W$ lying below (above) its q quantile given that $\hat{\boldsymbol{U}}_S$ lies above (below) its $1 - q$ quantile for $q \le 1/2$ $(q > 1/2)$. Fig. 2 (b) shows the difference in corresponding left and right quantile dependence illustrated in Fig. 2 (a) with a corresponding 95% confidence interval.

for later comparisons. A brief overview of these copula models is provided in Appendix A. The estimation results for the proposed constant copulas are given in Table 3, together with GoF test results. Among the constant copulas we consider, it is only the Gaussian and Student t that allow for negative dependence. To deal with this issue, we have performed suitable rotations of our data when estimating the Clayton, Gumbel, Joe-Frank and Symmetrized Joe-Clayton (SJC) copulas. Furthermore, the Gaussian and the Student t copulas are symmetric, the Clayton and Gumbel are asymmetric, and the combinations Joe-Frank and SJC allow for more flexible dependence structures and nest the case of symmetric dependence.

The GoF results in Table 3 support our earlier findings in Section 3.2. The Gaussian and Student t copulas are, according to all tests, a good specification. Clayton is rejected by all tests, while Gumbel is only partly rejected. For the combination copulas, the test results are more surprising: The Joe-Frank specification is accepted by all tests, while the SJC specification is rejected by all tests. We attempt to understand these results by plotting the quantile dependence we observe in our data together with the quantile dependence implied by some of the fitted copulas in Fig. 3.

We observe that the quantile dependence implied by the Gaussian copula provides a reasonable fit to our data. So does the Joe-Frank copula, by providing a fit that generates almost no asymmetry. The Gumbel copula on the other hand is too asymmetric, producing large deviations as we approach one of the tails. Lastly, the SJC, although implying less asymmetry than Gumbel, assigns too much probability to extreme events compared to what we observe in the data, and thus produces large deviations as we approach both tails.[9]

3.4. Time-varying copula models

To confirm our suspicion that the dependence of spot electricity prices and wind power production is time-varying, we perform the two tests briefly described in Section 2.3. The results are given in Table 4, showing no evidence of a one-time break in the dependence structure, but strong evidence for the presence of autocorrelation in the rank correlations.

In light of these findings, we consider three copula models where the transformed dependence parameter denoted by g evolves according to a GAS(1,1) model, see Eq. (12). The transformations applied to the copula dependence parameters, estimation and GoF test results are all displayed in Table 5. For the Gaussian copula, a closed form expression for the Fisher information can be derived (see e.g. Schepsmeier and Stöber, 2014). For the Gumbel and the Joe-Frank copulas, the Fisher information is computed numerically by performing the steps in Section 2.3.1. The Joe-Frank copula has two dependence parameters, and we consider the case where one parameter evolves according to the GAS specification, while the other is kept constant. It should however be mentioned that letting both parameters vary through time provides very little improvement. Regarding the parameter estimates, α is high in all models, implying a very persistent time-varying correlation process. Also, the intercept parameter ω is not significant in any model. As far as the GoF test results are concerned, the Joe-Frank and Gaussian GAS models are accepted at a 5% level, while the Gumbel GAS model is only partially accepted.

To visualize and compare the fits of the proposed GAS models, we plot the conditional rank correlation implied by the fitted time-varying copula models in Fig. 4 (a). The numbers are obtained by mapping the copula parameter(s) to a rank correlation coefficient[10]. In Figs. 4 (b)–(d) we plot actual 60-day rolling rank correlations of the data $(\hat{\boldsymbol{U}}_W, \hat{\boldsymbol{U}}_S)'$ together with the in-sample fit of the proposed time-varying models. To perform the same comparison for the out-of-sample period, we obtain the approx. uniforms $\left(\hat{\boldsymbol{U}}_W^{OOS}, \hat{\boldsymbol{U}}_S^{OOS}\right)'$ by first applying the estimated function for removing seasonality and then the ARMA–GARCH filters, without re-estimating any parameters, to the out-of-sample wind power production data and the out-of-sample spot electricity price data. The 60-day rolling rank correlations of $\left(\hat{\boldsymbol{U}}_W^{OOS}, \hat{\boldsymbol{U}}_S^{OOS}\right)'$ are then computed and compared to one-step-ahead forecasts from the time-varying copulas. Due to the elevated computational cost of using a rolling estimation window to produce forecasts, we restrict ourselves to considering a fixed estimation window corresponding to the in-sample period, but enlarge the conditioning set as information becomes available.

One first and surprising remark regarding Fig. 4 is related to the data itself and implicitly the fits produced by the GAS models, namely that the correlation is generally stronger during winter than during summer. There are many factors that can help explain this finding

[9] We have omitted the quantile dependence implied by the Student t and Clayton copulas in Fig. 3 for clarity reasons. The Student t copula implies quantile dependence coefficients that are almost indistinguishable from the Gaussian ones, which is due to the very high value we estimate for the degree of freedom of this copula. The Clayton copula implies even more asymmetry than Gumbel in the far right side of the quantile plot.

[10] Specifically, we follow the procedure described in Patton (2013): (1) construct a grid of copula parameters, (2) perform 100,000 simulations from the copula model at each point in the grid, (3) compute the rank correlation of the simulations, and finally (4) use linear interpolation to obtain the correlation at intermediate points. We also mention that the functions mapping the copula parameters to rank correlation are smooth.

Table 3
Estimation and GoF test results for constant copula models. The *p*-values less than 0.05 are given in italics, highlighting that the dependence structure is not well-represented by the proposed copula model. The superscript (*C*) refers to the tests performed on the empirical copula of the standardized residuals and the superscript (*R*) refers to the tests performed on the empirical copula of the Rosenblatt transforms. The GoF tests are simulation based (999 bootstraps) and take parameter estimation errors into account.

Copula		Parameter estimates	(s.e.)	log $\mathcal{L}$	GoF tests *p*-val.			
					Kolmogorov–Smirnov		Cramer–von Mises	
					$KS^{(C)}$	$KS^{(R)}$	$CvM^{(C)}$	$CvM^{(R)}$
Gaussian	$\hat{\rho}$	−0.4923	(0.0134)	355.07	0.4545	0.6096	0.6747	0.4044
Student *t*	$\hat{\rho}$	−0.4967	(0.0147)	357.15	0.4134	0.7427	0.7227	0.5435
	$\hat{\nu}^{-1}$	0.0318	(0.0170)					
Clayton	$\hat{\theta}$	0.7024	(0.0339)	288.94	*0.0020*	*0.0060*	*0.0000*	*0.0020*
Gumbel	$\hat{\theta}$	1.4455	(0.0220)	331.14	*0.0450*	0.0681	*0.0390*	0.0661
Joe-Frank	$\hat{\theta}$	8.8682	(4.4760)	368.77	0.7778	0.9359	0.7017	0.8278
	$\hat{\delta}$	0.3431	(0.1125)					
SJC	$\hat{\tau}^U$	0.3355	(0.0368)	320.18	*0.0070*	*0.0150*	*0.0230*	*0.0290*
	$\hat{\tau}^L$	0.2012	(0.0408)					

since price formation is a complex process that is not only influenced by supply and demand (which in turn have strong seasonal components), but also transmission capacity. To provide a few facts that can help explain our findings, we mention that the wind power production relative to the consumption in the DK1 price area has been higher for winter periods than summer periods, during the sample period we consider in this paper. Also, we can expect that situations with little wind during summer do not always push the prices upwards. This is (aside from consumption being lower during summer) due to the fact that DK1 is well connected with cables to Norway, Sweden and Germany, which are all heavy producers of renewable energy, and hence electricity could be imported at a lower price compared to the cost of having to turn on the more costly power stations in DK1.

Considering now the fits implied by the proposed time-varying copulas, Fig. 4 reveals that the Gaussian GAS implies most variation in the correlation and is able to capture periods with weaker dependence the best. The Gumbel GAS specification is the one that least captures the variation that we observe in the data. The Joe-Frank GAS specification is superior at reaching the stronger correlations, but does not produce correlations that are weaker than around −0.3. The plots clearly help establish that the Gumbel GAS specification is the inferior choice. However, it is difficult to choose the better copula when considering the Gaussian GAS against the Joe-Frank GAS.

From fitting not only time-varying copulas but also constant ones, we have so far obtained many different models that are actually

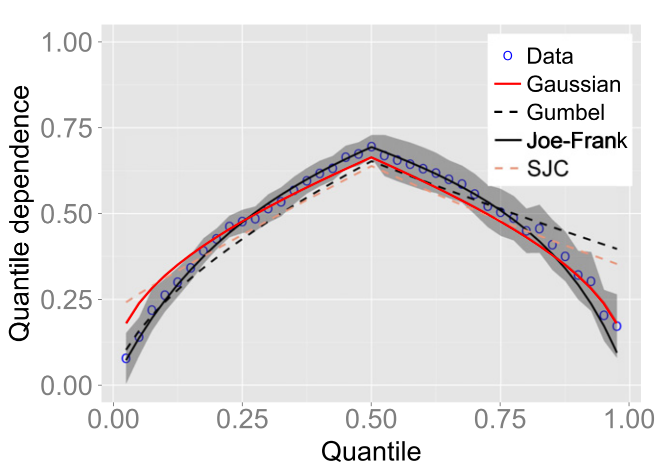

Fig. 3. Quantile dependence implied by some of the fitted constant copula models in Table 3.

well-specified according to the GoF tests. To help choose among all the considered copulas, we perform the pairwise comparison tests described in Section 2.5.[11] The results are summarized in Table 6. We find that The Joe-Frank GAS specification outperforms all other specifications in-sample, however its superiority over the Gaussian GAS specification is not statistically significant. When considering the out-of-sample results, the situation reverses, with the Gaussian GAS specification performing the best, but not significantly better than the Joe-Frank GAS. Since the Gaussian GAS is the smaller model, we will choose this specification as our preferred one, and continue our investigations using this model to describe the dependence between wind power production and spot electricity prices.

4. A simulation study

Performing simulations from a copula model is straightforward. The basic steps are (1) at time t, generate the pair $(U_{W,t}, U_{S,t})$ from the Gaussian copula with dependence parameter ρ_t, (2) perform the inverse of the transformations given in Eqs. (25) and (26) to obtain standardized residuals $(\eta_{W,t}, \eta_{S,t})$, (3) insert the standardized residuals in the marginal models from before (see Table 1) to obtain a deseasonalized pair $(\tilde{Y}_{S,t}, \tilde{Y}_{W,t})$, (4) use the estimated seasonal function to obtain a pair $(Y_{S,t}, Y_{W,t})$ of spot electricity price and wind power production, (5) compute ρ_{t+1} using the Gaussian GAS update equation and (6) repeat steps (1)–(5). Using this procedure one day at a time, we can construct spot electricity price series and wind power production series; and by repeating the process many times, an empirical distribution is produced. Such an empirical distribution is shown in Fig. 5.

Fig. 5 illustrates the simulated conditional joint distribution for December 2013 obtained by simulating 10,000 random paths for a one-month horizon. Note that although we have chosen a Gaussian copula model for the dependence structure, the marginal distributions were chosen to be a skewed generalized error distribution and a skewed t distribution for the wind power production and spot electricity prices, respectively. Therefore, the resulting joint distribution is not bivariate normal; as illustrated in Fig. 5, the simulated distribution exhibits asymmetry and heavy tails.

We will now use our model to study how different wind scenarios affect the distribution of prices. To this end, we perform one-month ahead simulations for all OOS months, i.e. a total of 24 months. Due to the elevated computational cost, we do not re-estimate the

[11] The in-sample pairwise comparison between the Gaussian and the Student t copula is based on a simple t-test, since these models are nested.

Table 4
Test results for time-varying dependence. To test for the presence of a one-time break in the rank correlation we use the "sup" test, and test the null of no one-time break. To test for the presence of time-varying dependence of autoregressive type we consider the regression $\hat{U}_{W,t}\hat{U}_{S,t} = \mu + \sum_{i=1}^{p} \phi_i \hat{U}_{W,t-i}\hat{U}_{S,t-i} + \varepsilon_t$, for $p = 1, 5, 7$; the null of a constant copula cannot be rejected if we find that $\phi_i = 0$, for $i = 1, \ldots, p$. For all tests, p-values are obtained by bootstrap testing (based on 999 bootstraps, where bootstrap samples are obtained by randomly drawing rows, with replacement, from $(\hat{\boldsymbol{U}}_W, \hat{\boldsymbol{U}}_S)'$).

	One-time break	Time-varying dep. of autoreg. type		
		AR(1)	AR(5)	AR(7)
p-Value	0.7898	0.0020	0.0110	0.0000

parameters of our joint model; we do however enlarge the conditioning set one month at the time. In Fig. 6 (a)–(b), we display simulated empirical price distributions conditional on different levels of low/high wind scenarios. The simulations are grouped into winter (Dec., Jan., Feb.) and summer (Jun., Jul., Aug.) months. To define what a low/high wind scenario is during winter, we have considered the 20% and 80% quantiles of our actual OOS wind power production data during the specified winter months; the same procedure was followed for the summer months. For both the winter and the summer period, we observe that the different wind scenarios shift the simulated price distributions. Moreover, the simulated distributions are left-skewed for the high wind scenarios (the skewness parameter is −1.98 for the winter months and −1.03 for the summer months), implying that extreme low prices are more likely than extreme high prices. For the low wind scenarios, the estimated distributions are right-skewed (the skewness is 0.64 and 1.06 for the winter and summer months respectively), thus implying the opposite compared to the high wind cases. We also notice that the low/high wind scenarios push the price distributions further apart for the winter months than the summer months, which we have confirmed by measuring the Kullback–Leibler distance between distributions. This can be explained by the fact that during summer periods, the dependence between electricity prices and wind power production is weaker than during winter periods, as earlier illustrated in Fig. 4. All these features are present when performing the same calculations on the actual data, which we show in Fig. 6 (c)–(d), confirming that our empirical model captures the dynamics between daily spot electricity prices and wind power production.

5. Application to pricing and risk management

In the following, we present applications of the proposed joint model for spot electricity prices and wind power production. We start by consider an energy trading company that enters into agreements with wind power producers, where a predetermined fixed price R is paid for the fluctuating wind power production. Since the production will first become known through the delivery period of the agreements, these products imply a volumetric risk. Furthermore, we assume that the trading company sells the production it receives from the wind power producers on the day-ahead market, at a spot price we denote by S. Hence, the company will also be exposed to price risk. In the remaining of this section, we will refer to such agreements as fixed price for fluctuating wind power production agreements. With such a formulation, we can express the profit of the trading company as

$$\sum_{t=T_1}^{T_2} Q_t(S_t - R), \tag{27}$$

where time is measured in days, Q_t is the wind power production at time period t, S_t is the daily spot electricity price valid at t, and R is a fixed price set at the inception of the contract, which we denote t_0. Furthermore, the contract length spans from T_1 to T_2, where $t_0 < T_1 \leq T_2$. We note that to participate in the day-ahead electricity auction market, buy or sell bids have to be made to the exchange one day before delivery takes place. By working with the payoff in Eq. (27), we implicitly assume that the quantity we bid one day before equals the actual wind power production, i.e.

$$Q_t = \mathbb{E}_{t-1}[Q_t], \tag{28}$$

where $\mathbb{E}_{t-1}[Q_t]$ denotes the expectation at time $t-1$ for the production at time t. Thus, we assume no balancing risk.

What differentiates the product described above with payoff given in Eq. (27) from a standard forward contract is the production uncertainty associated with the former, and hence the presence of an additional risk due to the correlation between S and Q. If we express the price R in terms of the forward price F, Eq. (27) becomes

$$\sum_{t=T_1}^{T_2} Q_t(S_t - (F - c)), \tag{29}$$

where $F \equiv F(t_0, T_1, T_2)$ denotes the forward price at time t_0, for the delivery period from T_1 to T_2 and $c \equiv c(t_0, T_1, T_2)$ denotes the compensation that is to be subtracted from the forward price due to the negative correlation between prices and volume. So c can be thought of as the price of correlation risk. The fair value of c can be obtained by the usual practice of setting the discounted conditional expectation of the payoff given in Eq. (29) equal to zero. To ease the presentation, we will assume a risk-free rate of zero, thus obtaining:

$$\mathbb{E}_{t_0}^{\mathbb{Q}}\left[\sum_{t=T_1}^{T_2} Q_t(S_t - (F - c))\right] = 0, \tag{30}$$

$$c = F - \frac{\mathbb{E}_{t_0}^{\mathbb{Q}}\left[\sum_{t=T_1}^{T_2} Q_t S_t\right]}{\mathbb{E}_{t_0}^{\mathbb{Q}}\left[\sum_{t=T_1}^{T_2} Q_t\right]}. \tag{31}$$

With our framework, an estimate for c can easily be obtained by performing Monte Carlo simulations from the proposed copula model.

Table 5
Estimation and GoF results for time-varying copulas. Due to the high computational time, the GoF tests and standard errors are based on 99 bootstraps. The superscript (R) indicates that the GoF tests are based on the Rosenblatt transform.

	Transf. h	Parameter estimates (s.e.)				$\log \mathcal{L}$	GoF tests p-val.	
		$\hat{\omega}$	$\hat{\alpha}$	$\hat{\beta}$	$\hat{\delta}$		$KS^{(R)}$	$CvM^{(R)}$
Gaussian	$\log\left(\frac{1+\rho}{1-\rho}\right)$	−0.0196	0.9820	0.0390	–	373.90	0.5354	0.4646
		(0.0268)	(0.0246)	(0.0159)				
Gumbel	$\log(\theta - 1)$	−0.0272	0.9672	0.0420	–	342.90	*0.0404*	0.0707
		(0.1527)	(0.1849)	(0.0334)				
Joe-Frank	$\log(\theta - 1)$	0.0314	0.9860	0.0403	0.2944	388.77	0.7959	0.8571
		(0.0509)	(0.0208)	(0.0127)	(0.0894)			

However, this estimate will reflect the price of correlation risk under the physical or objective measure $\mathbb{P}$, since the model is fitted to historical spot electricity price and wind power production data. According to Eqs. (30) and (31), the expectations must be taken under a pricing measure $\mathbb{Q}$, that will reflect the risk premium charged by, in our context, the energy trading company offering the "insurance" to the wind power producer. Following Benth et al. (2008), the pricing measure $\mathbb{Q}$ is equivalent to $\mathbb{P}$, but needs not be an equivalent *martingale* measure due to the non-storability of our underlying "assets". Since neither electricity nor wind can be stored, they are not tradable assets in the classical sense. This implies that the spot–forward relation, for example, cannot be derived based on a buy-and-hold hedging argument. Instead, the usual practice is to simply define the forward price as the conditional expectation of the spot electricity price under the risk-neutral probability measure $\mathbb{Q}$, thereby turning the discounted spot price into a martingale (see Benth and Meyer-Brandis, 2009 and Benth and Šaltytė Benth, 2012). Indeed, by defining

$$F(t_0,T_1,T_2)=\mathbb{E}_{t_0}^{\mathbb{Q}}\left[\frac{1}{T_2-T_1+1}\sum_{t=T_1}^{T_2}S_t\right], \tag{32}$$

for the case of electricity, one can compute the implied market price of risk by considering the difference between quoted forward prices in the market and forward prices obtained by simulation with our model under $\mathbb{P}$. For further discussions and empirical studies regarding pricing in electricity markets we refer to Benth et al. (2013), Burger et al. (2004), Kolos and Ronn (2008), and Lucia and Schwartz (2000). In theory, the same could be done to estimate the risk premium associated with wind, however forwards with wind index as underlying are not currently traded in most European energy markets — and if they are, they are highly illiquid.

The fact that our setting is a bivariate one complicates the question of measure change even further, since aside from the marginal behavior of spot electricity price and wind power production under $\mathbb{Q}$, implied information regarding the market price of dependency risk must also be provided. A parametrization of this is not straightforward; in fact, the discussion can become quite extensive in the context of copulas and incomplete markets. Such a discussion is outside the scope of this paper, and we refer instead to Cherubini et al. (2004) for more details. Moreover, even if a theoretical procedure to calibrate the market price of dependency risk were to be established, the lack of exchange-traded instruments written on spot times wind would impede applying this in practice.

In light of the above discussion, we turn to the rational expectation hypothesis, which is a valid choice and a common assumption in this context (see e.g. Benth and Kettler, 2011 , Coulon et al., 2013 , and Oum and Oren, 2010). This implies that we set $\mathbb{P}=\mathbb{Q}$, i.e. set the market price of risk to zero. Since we suspect a measure change to yield different prices, but not to alter the overall conclusions in our following empirical analysis, we find this assumption to be a reasonable one.

According to the payoff in Eqs. (27) or (29), it is clear by now that we are dealing with two sources of risk simultaneously: one is related to price uncertainty, and the other is related to production uncertainty; and since the market is incomplete, a perfect hedge cannot be performed. However, the price risk can be hedged. Here, we construct a simple hedging portfolio by taking a short position in a quantity H^* of standard forward power contracts. We assume that the hedge is static and performed at time t_0. The payoff of the hedge for the entire delivery period is given by

$$H^*\left(\mathbb{E}_{t_0}^{\mathbb{Q}}\left[\frac{1}{T_2-T_1+1}\sum_{t=T_1}^{T_2}S_t\right]-\frac{1}{T_2-T_1+1}\sum_{t=T_1}^{T_2}S_t\right), \tag{33}$$

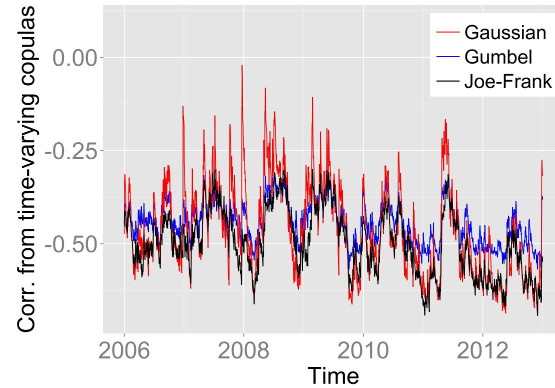

(a) Conditional rank correlation implied by time-varying copulas

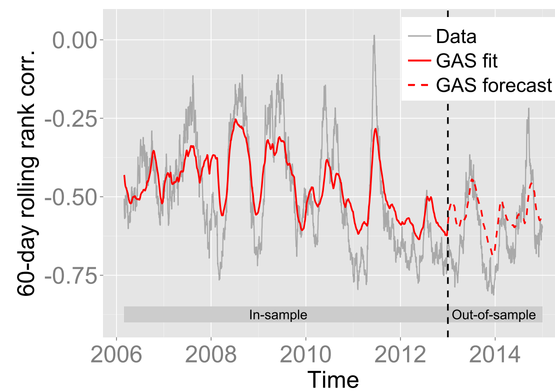

(b) Gaussian copula

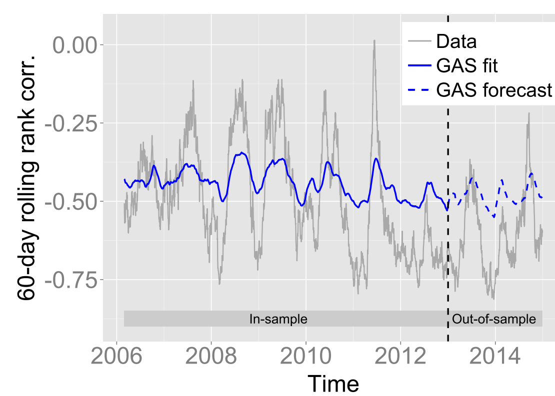

(c) Gumbel copula

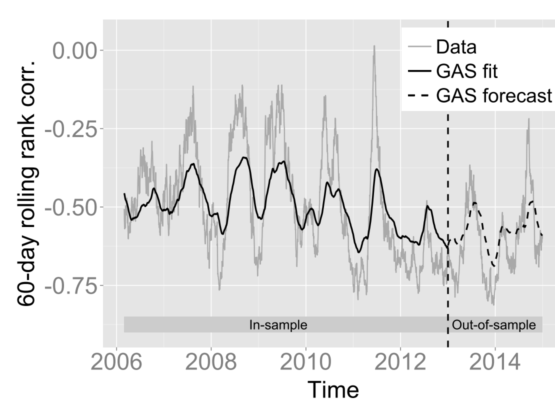

(d) Joe-Frank copula

Fig. 4. Fits and forecasts produced with the three time-varying copulas from Table 5.

Table 6
t-Statistics from in-sample and out-of-sample pairwise model comparisons. A positive (negative) value means that the model in the row is superior (inferior) to that in the column. t-Statistics are followed by *, ** or *** if one model is significantly better than the other at a 0.1, 0.05 or 0.01 significance level, respectively. The in-sample model comparisons are based on Rivers and Vuong (2002) and the out-of-sample model comparisons are based on Diks et al. (2010).

	Gaussian	Student t	Clayton	Gumbel	Joe-Frank	SJC	Gaussian^{GAS}	Gumbel^{GAS}	Joe-Frank^{GAS}
*In-sample model comparisons*Gaussian									
Student t	1.88^{*}								
Clayton	-4.61^{***}	-5.04^{***}							
Gumbel	-2.20^{**}	-2.71^{***}	7.07^{***}						
Joe-Frank	1.40	1.28	5.27^{***}	3.10^{***}					
SJC	-3.91^{***}	-4.91^{***}	3.32^{***}	-1.74^{*}	-3.54^{***}				
Gaussian^{GAS}	2.94^{***}	2.54^{***}	5.71^{***}	3.63^{***}	0.44	5.30^{***}			
Gumbel^{GAS}	-1.12	-1.42	8.08^{***}	2.91^{***}	-2.00^{**}	3.07^{***}	-2.91^{***}		
Joe-Frank^{GAS}	3.14^{***}	3.12^{***}	6.37^{***}	4.44^{***}	3.20^{***}	4.88^{***}	1.57	3.66^{***}	
log $\mathcal{L}$	355.06	357.13	288.93	331.14	368.77	320.17	373.90	342.90	388.77
Out-of-sample model comparisons									
Gaussian									
Student t	1.41								
Clayton	-4.36^{***}	-4.95^{***}							
Gumbel	-1.58	-2.04^{**}	8.18^{***}						
Joe-Frank	0.16	-0.22	3.64^{***}	1.32					
SJC	-2.67^{***}	-3.43^{***}	5.19^{***}	-1.99^{**}	-1.99^{**}				
Gaussian^{GAS}	2.85^{***}	2.76^{***}	5.61^{***}	3.54^{***}	2.04^{**}	4.56^{***}			
Gumbel^{GAS}	-0.67	-0.96	6.53^{***}	2.22^{**}	-0.63	2.53^{***}	-2.75^{***}		
Joe-Frank^{GAS}	1.76^{*}	1.58	4.21^{***}	2.38^{***}	2.46^{***}	2.90^{***}	-0.29	1.82^{*}	
log $\mathcal{L}$	160.10	161.48	129.55	150.52	160.67	146.11	171.96	155.25	170.56

or in a compact form

$$H^{*}(F-\bar{S}), \tag{34}$$

where F denotes the same forward price as in Eq. (29), and $\bar{S}$ denotes the average day-ahead electricity price for the same delivery period. To obtain H^{*}, we fix c to its value obtained from Eq. (31) and follow the standard procedure of minimizing the variance of the portfolio payoff:

$$\min_{H^{*}} \mathbb{V}\mathrm{ar}_{t_0}\left[\sum_{t=T_1}^{T_2} \tilde{Q}_t(S_t-(F-c))+H^{*}(F-\bar{S})\right]. \tag{35}$$

In Eq. (35), $\tilde{Q}_t = 24 \cdot Q_t \cdot \Lambda$, with Λ being the total installed capacity under the agreement that pays out a predetermined fixed price

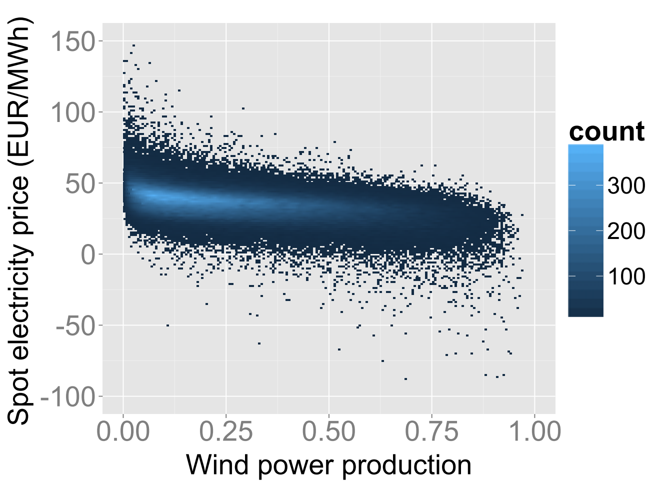

Fig. 5. Simulated joint distribution for the daily spot electricity prices and the wind power production in December 2013. The results are based on 10,000 simulations (for each day of December) and a Gaussian GAS model for the dependence structure.

in return for the fluctuation wind power production. Since Q_t corresponds to daily wind power production relative to the total installed capacity in the entire DK1 price area, we need to transform this number to daily wind power production measured in MWh corresponding to the total installed capacity that the energy trading company actually has under agreement. By performing this transformation, we imply that our joint model is a good representation on a smaller scale. This is a realistic assumption as long as the energy trading company manages a portfolio of diversified wind turbines in terms of type and location. Solving for H^{*} in Eq. (35) yields

$$H^{*} = \frac{\mathbb{C}\mathrm{ov}_{t_0}\left[\bar{S}, \sum_{t=T_1}^{T_2}\tilde{Q}_t S_t\right]-(F-c)\mathbb{C}\mathrm{ov}_{t_0}\left[\bar{S}, \sum_{t=T_1}^{T_2}\tilde{Q}_t\right]}{\mathbb{V}\mathrm{ar}_{t_0}\left[\bar{S}\right]}. \tag{36}$$

It is clear that by hedging a quantity that is equal to H^{*}, we are protected on average and not against worst case scenarios, such as the combination of extremely low prices/high wind power production, which is a probable outcome in the DK1 price area. We could remedy the situation to a large extent by adding options to our portfolio, however this is outside the scope of the present paper. Work related to the optimal hedging of volumetric risk associated with wind power production is, to the best of our knowledge, not yet available. However, energy related discussions regarding the hedging of volumetric risk associated with consumers' load are presented in e.g. Oum and Oren (2009) and Oum et al. (2006), where many of the ideas can be transferred to our application. Nonetheless, our simple hedge is actually realistic since the market for options is very illiquid in DK1.

5.1. Example 1

Having developed a joint model for day-ahead electricity prices and wind power production, we can perform Monte Carlo simulations and use Eq. (31) to find the fair fixed price/compensation of a contract with any given specifications. Assume that we stand on the last trading day of November 2013, denoted t_0, and wish to find the fixed price for a front month contract, namely a December 2013

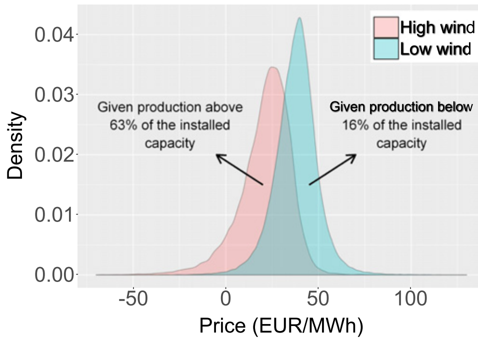

(a) Simulated prices: winter period

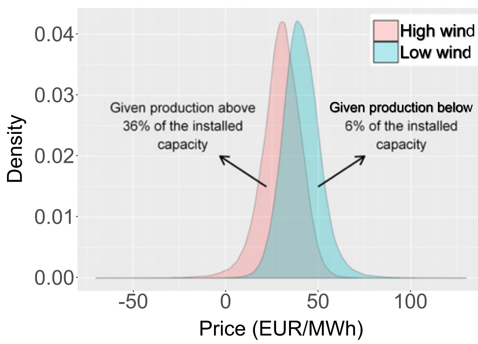

(b) Simulated prices: summer period

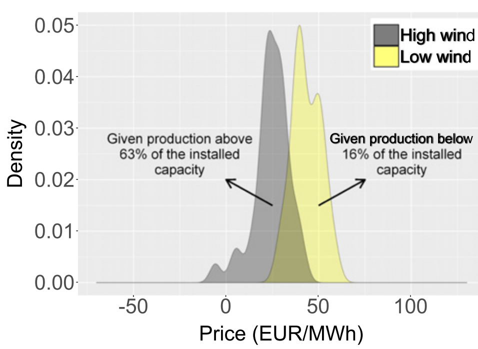

(c) Actual prices: winter period

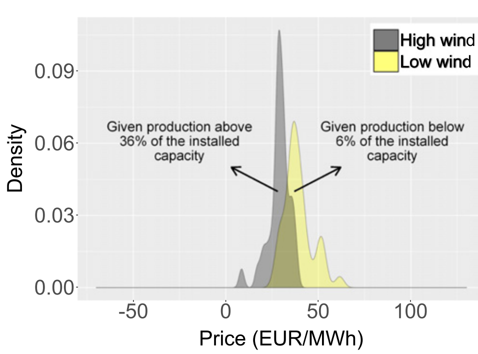

(d) Actual prices: summer period

Fig. 6. Distributions for the daily spot electricity prices during winter and summer months, for the out-of-sample period 01/01/2013 to 31/12/2014, under the assumption of high and low wind power production. The simulated predictive distributions are based on 10,000 one-month-ahead simulations, using a Gaussian GAS model for the dependence structure. Fig. 6 (c) and (d) are based on 37 observations. To define the percentage corresponding to high/low wind scenarios during winter and summer, we used the 0.20 and 0.80 quantiles of the actual out-of-sample wind power production data.

Table 7
Simulation results for a December 2013 contract, with valuation date 29 November 2013, i.e. one business day before start delivery of the contract. The results are based on 10,000 simulations and using a Gaussian GAS model for the dependence structure.

Contract information		
Time of valuation	t_0	29/11/2013
Contract length	T_1 to T_2	01/12/2013 to 31/12/2013
Pricing results		
Simulated forward price	$F \equiv F(t_0, T_1, T_2)$	35.26 EUR/MWh
Price of correlation risk	$c \equiv c(t_0, T_1, T_2)$ cf. Eq. (31)	3.24 EUR/MWh
Fixed price for fluctuating wind power production	$R \equiv R(t_0, T_1, T_2)$	32.02 EUR/MWh
Risk management results (500 MW installed capacity under agreement)		
5 % VaR without price hedge	See Fig. 7	1,099,248 EUR
5 % VaR with price hedge	See Fig. 7	465,485 EUR

contract. Given all information available up to and including the valuation date t_0, we perform 10,000 simulations for price and quantity from our proposed joint model, where for each simulation we keep a path of length 31 (since we work with daily data) corresponding to the number of days in December. We note that we work with a fixed estimation window corresponding to the IS period, but enlarge the filtration, conditioning on the information up to and including the valuation date t_0. The contract specifications and results are summarized in Table 7, and we see that due to the negative correlation between prices and production, the compensation c that is to be subtracted from the forward price equals 3.24 EUR/MWh.

In addition to calculating the fixed price of a contract with fluctuating wind power production, we can extract information from the performed simulations that can be useful in a risk management context. We assume that agreements corresponding to an installed capacity of 500 MW are entered into on the last trading day of November 2013, with delivery December 2013. The price of a standard forward contract is fixed to its estimated value of 35.26 EUR/MWh, and the price of an agreement with a fluctuating wind

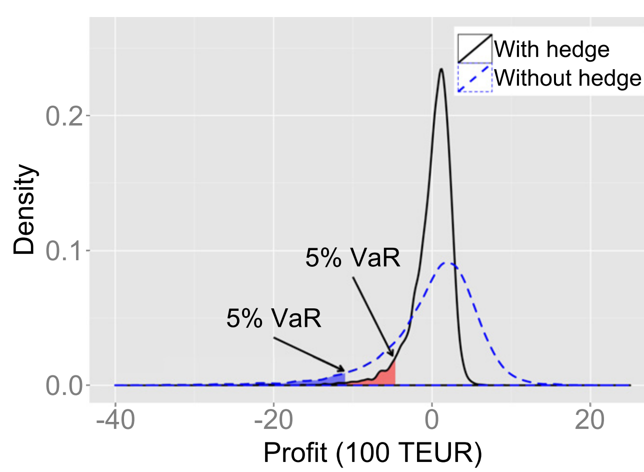

Fig. 7. Profit distributions for a December 2013 contract. The results are based on 10,000 simulations of price and quantity, using a Gaussian GAS model for the dependence structure. The forward price is fixed to 35.26 EUR/MWh, the compensation is fixed to 3.24 EUR/MWh and the total installed capacity of the portfolio equals 500 MW. The variance minimizing hedge quantity H^* is obtained by performing the calculation in Eq. (36).

power production is set to 32.02 EUR/MWh cf. Table 7. Given these specifications, we estimate the distribution of the portfolio payoff (see Fig. 7) and calculate the 5% Value-at-Risk (see Table 7) in two cases: One where the portfolio includes a price hedge, and one without a price hedge. When covering our price exposure in the forward market by assuming a short position corresponding to a quantity of H^{*} forwards, we observe that the variance of the profit distribution reduces significantly. In this example, the 5% Value-at-Risk is reduced from approximately EUR 1.1 million to EUR 0.5 million. It is also important to notice that the profit distribution is in both cases asymmetric, with a heavy-tail to the left, translating to the fact that expected losses are greater than expected gains.

Revisiting the issue of pricing and considering the profit distributions in Fig. 7, alternative approaches to that of performing a measure change can be applied. An example can be to consider an a priori given 5% Value-at-Risk level that is acceptable, and solve for the correlation risk premium that satisfies this level.

To stress the effect of correlation on the profit distribution, we perform additional simulations, where all but the copula model remains unchanged. Specifically, we assume the independence copula and thus a zero compensation, instead of the Gaussian GAS model which we have established reflects the reality to a much greater extent. Fig. 8 (a) illustrates the estimated profit distributions of the portfolio (with no hedge), and shows that the negative correlation implies a distribution that is more asymmetric. If prices and production were independent, we estimate a 5% Value-at-Risk of EUR 0.93 million corresponding to a reduction of approximately 15% compared to the 5% Value-at-Risk of EUR 1.1 million we obtain with the Gaussian GAS copula. Assuming independence would thus lead to an underestimation of risk. We also display the average spot electricity price for the period of the contract as a function of the estimated profit in Fig. 8 (b). Under independence, we observe that the payoff becomes linear, and hence forwards would suffice as hedging instruments. Under negative dependence, the payoff becomes non-linear, emphasizing the need for options in the hedging portfolio. Furthermore, we observe that a larger profit (smaller loss) can be obtained if prices and production are independent as we move away from the mean average price of 35.26 EUR/MWh. This is also supported by Fig. 8 (a), where we observe that the negative correlation implies that a smaller probability is assigned to large profits, and a higher probability is assigned to large losses.

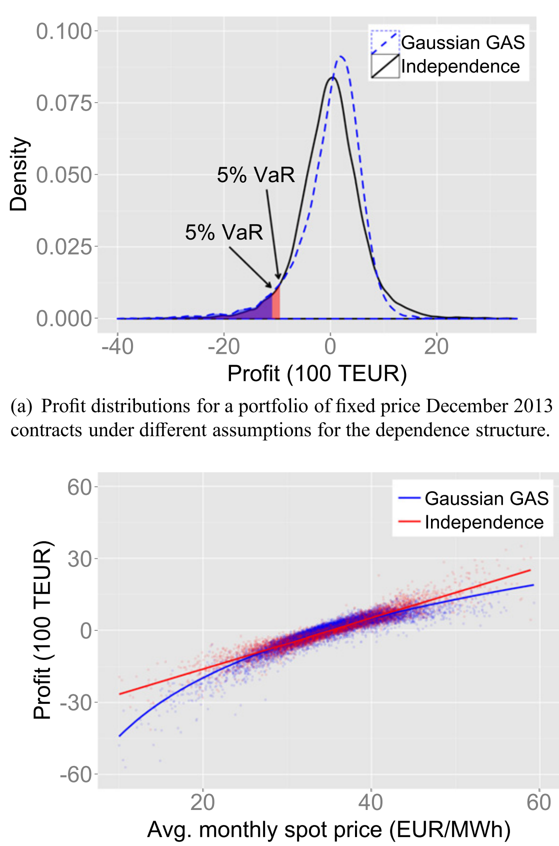

(a) Profit distributions for a portfolio of fixed price December 2013 contracts under different assumptions for the dependence structure.

(b) Estimated payoffs for a portfolio of fixed price December 2013 contracts, as a function of the avg. monthly spot electricity price.

Fig. 8. Illustration of the importance of correlation in the analysis of profit. The results are based on 10,000 Monte Carlo simulations with a Gaussian GAS copula (c is fixed to 3.24 EUR/MWh) and the independence copula (c is fixed to 0 EUR/MWh), respectively. The total installed capacity of the portfolio is set to 500 MW, and the same marginal models for prices and wind power production are used.

5.2. Example 2

In Section 3.4, we have established that some of the fitted time-varying copula models are superior to the constant ones, see e.g. Table 6. Here, we wish to investigate if this also holds when comparing the actual profits or losses generated with different copula models. For this, we consider the OOS period corresponding to the years 2013 and 2014. We assume the following trading strategy: On the last trading day of each month (Dec. 2012–Nov. 2014), we enter into front month agreements with wind power generators, where a fixed price is paid for the fluctuating wind power production. The total installed capacity of each monthly portfolio is fixed to 500 MW. We perform 10,000 simulations from joint models with the different copula specifications that we wish to compare against each other (marginal models are kept unchanged), and estimate compensations c and hedge quantities H^{*} for each month at a time using Eqs. (31) and (36). For each monthly portfolio, we then calculate the realized profit using the actual daily electricity prices, actual daily wind power production[12] and actual forward prices.

For clarity, let us consider a concrete example: We stand on the last trading day of December 2012, and wish to enter into fixed price agreements with fluctuating wind power production for the January 2013 month. To enter the contract, we first estimate the fixed price that we are willing to pay for the production that we will receive during January. Since we also perform a hedge in the forward market, we estimate the quantity of forwards we are to short. In this example, we will use a constant Clayton copula to describe the dependence between prices and wind power production, and hence we obtain an estimated compensation denoted by $\hat{c}^{\text{Clayton}}_{t_0,\text{Jan}}$ and an estimated hedge quantity $\hat{H}^{*,\text{Clayton}}_{t_0,\text{Jan}}$. On the last trading day of December 2012, we can observe the actual forward price $F^{\text{Obs}}_{t_0}$, and thus the fixed price we offer the wind power producers is

$$\hat{R}^{\text{Clayton}}_{t_0,\text{Jan}} = F^{\text{Obs}}_{t_0} - \hat{c}^{\text{Clayton}}_{t_0,\text{Jan}}. \tag{37}$$

By the end of January 2013, we will also have observed the actual daily spot electricity prices S^{Obs} and the actual daily wind power production Q^{Obs} for the DK1 price area. With this information, we can

[12] The actual daily wind power production is given in % for the entire price area, but only a subset of the existing wind turbines in DK1 is part of our portfolio. Therefore, we note that the realized profit we calculate is an approximation; we obtain the actual production of the wind turbines under agreement by multiplying the actual daily wind power production for the entire price area with the assumed installed capacity of the portfolio of 500 MW and 24 h.

Table 8
OOS model comparisons based on realized monthly profit/loss. In the first column block, we calculate how often each copula model yields the lowest monthly loss or the highest monthly profit. The second column block presents the realized average profit/loss (in EUR/MWh) for selected copula models, obtained by dividing the total realized cash-flow for the period by the total realized wind power production. All results are based on the same trading strategy and 10,000 simulations.

	Highest profit (lowest loss) per month for the OOS period		Realized average profit for the OOS period (EUR/MWh)	
	Constant	Time-varying (GAS)	Constant	Time-varying (GAS)
Gaussian	4.16%	**62.50%**	−0.9144	−**0.6103**
Gumbel	16.67%	0.00%	−0.8693	−0.7961
Joe-Frank	0.00%	16.67%	−1.0294	−0.6666
Clayton	0.00%	–	−1.1465	–

now approximate the actual profit resulting from the trades we have performed:

$$\text{Actual profit}_{\text{Jan}} = \underbrace{\sum_{t=T_1}^{T_2} \tilde{Q}_t^{\text{Obs}} \left(S_t^{\text{Obs}} - \hat{R}_{t_0\,\text{Jan}}^{\text{Clayton}}\right)}_{\text{Agreement payoff}} + \underbrace{\hat{H}_{t_0\,\text{Jan}}^{*,\text{Clayton}} \left(F_{t_0}^{\text{Obs}} - \bar{S}^{\text{Obs}}\right)}_{\text{Hedge payoff}} \tag{38}$$

where $t_0 = 31/12/2012$, $T_1 = 01/01/2013$, $T_2 = 31/01/2013$ and $\tilde{Q}^{\text{Obs}}$ is the approximation

$$\tilde{Q}_t^{\text{Obs}} = Q_t^{\text{Obs}} \cdot 24(\text{h}) \cdot 500(\text{MW}). \tag{39}$$

The results obtained by performing the above calculations for all OOS months with different copula specifications are presented in Table 8. The numbers show that the joint model with a Gaussian GAS copula provides the highest (lowest) monthly profit (loss) in 15 out of the 24 months, corresponding to 62.50%. Considering the second column block of Table 8, we see that it is indeed the Gaussian GAS and the Joe-Frank GAS that yield the lowest losses in average, which supports the results we obtained in Section 3.4. Hence, allowing for time variation in a suitable copula model is beneficial. The constant Clayton specification performs the poorest, generating the largest average loss. This is again in accordance with earlier findings, where we have established that the constant Clayton specification is not suitable for the dependence of prices and wind power production, and also least suitable among the copula models we consider in Table 8. The time-varying Gaussian and Joe-Frank copulas outperform the other copulas since they are able to capture the increasingly negative correlation we observe towards the last years of our sample (see Fig. 4); and thus, they are able to generate larger compensations. For instance, the constant Gaussian copula yields an average compensation for the OOS period of 2.69 EUR/MWh, while the Gaussian GAS copula yields a value of 2.98 EUR/MWh.

Lastly, we illustrate in Fig. 9 the evolution of actual forward prices and also the evolution of compensations estimated with our proposed joint model for electricity prices and wind power production, i.e. the one with the Gaussian GAS copula specification for the dependence structure.

Overall, compensations amount to an increasing percentage of the forward price during the period of our study. Clearly, this is mainly due to the decreasing tendency in forward prices, but also due to the slight increase in compensations if we consider the IS and OOS average compensations. The slight increase in compensations can be justified by the increasing installed capacity of wind power that Denmark has experienced over the past years — and hence the stronger dependence between wind power production and electricity prices. This also explains the decrease in forward prices, but only to a small extent; the major contributing factor here has been the decreasing raw material prices. The reduction in forward price due to the correlation risk amounts to an average of 7%, and can reach as high as 11%. A similar conclusion is reached by Elberg and Hagspiel (2015), where the authors study the market value of wind power at different locations in Germany, and show that this value is reduced compared to the average spot price as a result of increasing wind power penetration.

6. Conclusion

This work concentrates on the dependency between daily spot electricity prices and wind power production, and its role regarding the pricing and the risk distributions associated with contracts exposed to both price and volumetric risk. The analysis is carried out on data from the Danish power market, which is characterized by a

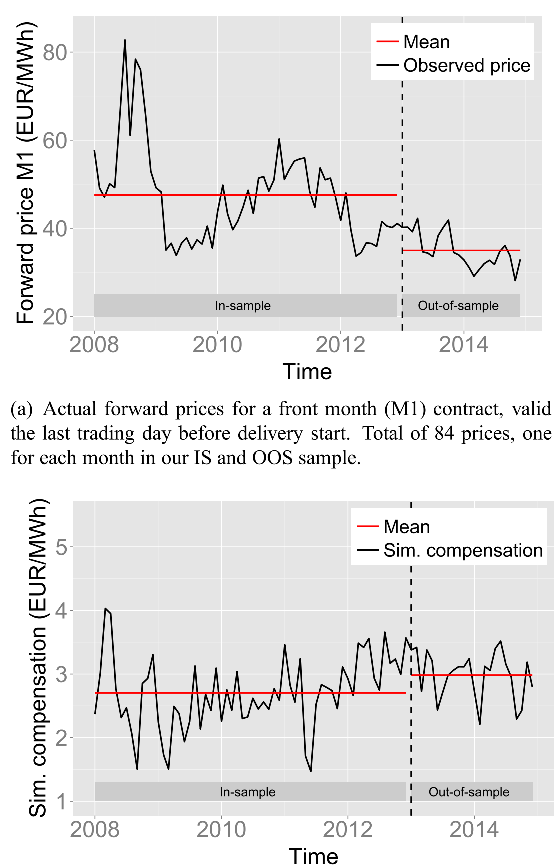

(a) Actual forward prices for a front month (M1) contract, valid the last trading day before delivery start. Total of 84 prices, one for each month in our IS and OOS sample.

(b) Simulated compensations for a front month contract, valued the last trading day before delivery start. The results are based on 10,000 simulations, with a Gaussian GAS models for the dependence structure.

Fig. 9. Evolution of actual forward prices and estimated compensations.

high penetration of wind power in the system. We propose a copula approach since we wish to concentrate on the dependence in more detail. We employ marginal models of the ARMA–GARCH type and parametric error distributions for each individual variable, and then link the innovations through various constant and time-varying copulas. Based on statistical tests concerning copula selection, we choose a time-varying Gaussian copula as our preferred specification for the dependence structure. By performing Monte Carlo simulation studies, we are able to visualize the joint empirical distribution implied by our model, and see how this deviates from the Gaussian benchmark. Also, we study the distribution of prices conditional on different levels of wind power penetration, and show that prices decrease (increase), on average, at times of high (low) levels of wind power production; the shape of the conditional distribution of prices is also affected by the different levels of wind power production. These findings confirm what previous studies concerned with the impact of wind power – or predicted wind power penetration – on electricity prices have shown (e.g. Gelabert et al., 2011, Jónnson et al., 2010).

We apply the developed empirical model in the context of an energy trading company offering wind power producers a predetermined fixed price for their fluctuating wind power production. We find that the correlation risk premium that the energy trading company should charge when entering such agreements is significant, amounting to 7% of the price of a standard forward power contract on average. Furthermore, our results indicate that the choice of copula impacts the price of correlation risk: An out-of-sample study based on comparing realized profits generated by different copulas shows that introducing time-variation in the copula model is beneficial. When considering the profit distribution, we find that under independence, the risk is underestimated. Additionally, we show that a simple hedge in the forward market can reduce e.g. the 5% Value-at-Risk of the profit distribution significantly. However, due to the non-linearity of profit, options should be included in the hedging portfolio in order to reduce the risk even further; this could be an interesting subject for further research.

Finally, although our empirical study concentrates on the Danish power market, the mechanism of spot price formation in e.g. other European electricity markets is also based on matching supply and demand. Further, wind power production has a very low marginal cost, ensuring that it will always be represented in the merit order stack. Due to the physical conditions upon which the day-ahead electricity markets are based, we believe that the proposed modeling framework is relevant and can be applied to other electricity markets that, like Denmark, rely heavily on wind power production. Such extensions are left for future research.

Acknowledgments

The authors would like to express their gratitude to Rikke Preisler Vilstrup for her contributions to this paper through a mutual unpublished master thesis project, and Thomas Aalund Fredholm, Christian Sønderup and Jakob Vive Munk at Neas Energy for posing the problem and providing helpful comments and suggestions. The authors also thank the referees for providing constructive criticism and suggestions that enhanced the quality of this paper.

Funding

Anca Pircalabu acknowledges support from Innovation Fund Denmark, grant number 4135-00082B.

Appendix A. Supplementary data

Supplementary data to this article can be found online at http://dx.10.1016/j.eneco.2016.11.023.

References

Alexander, C., 2004. Correlation in crude oil and natural gas markets. In: Kaminski, V. (Ed.), Managing Energy Price Risk: The New Challenges and Solutions. Risk Publications.

Avdulaj, K., Barunikl, J., 2015. Are benefits from oil-stocks diversification gone? New evidence from a dynamic copula and high frequency data. Energy Econ. 51, 31–44.

Benth, F.E., Biegler-König, R., Kiesel, R., 2013. An empirical study of the information premium on electricity markets. Energy Econ. 36, 55–77.

Benth, F.E., Kettler, P.C., 2011. Dynamic copula models for the spark spread. Quant. Finan. 11 (3), 407–421.

Benth, F.E., Meyer-Brandis, T., 2009. The information premium for non-storable commodities. J. Energy Markets 2 (3), 111–140.

Benth, F.E., Šaltytė Benth, J., 2012. Modelling and Pricing in Financial Markets for Weather Derivatives. World Scientific.

Benth, F.E., Šaltytė Benth, J., Koekebakker, S., 2008. Stochastic Modelling of Electricity and Related Markets. World Scientific.

Berg, D., 2009. Copula goodness-of-fit testing: An overview and power comparison. Eur. J. Financ. 15 (7-8), 675–701.

Bollerslev, T., 2008, Sep. Glossary to ARCH (GARCH). CREATES Research Papers 2008-49, School of Economics and Management, University of Aarhus.

Burger, M., Klar, B., Muller, A., Schindlmayr, G., 2004. A spot market model for pricing derivatives in electricity markets. Quant. Finan. 4 (1), 109–122.

Cherubini, U., Luciano, E., 2002. Bivariate option pricing with copulas. Appl. Math. Finance 9, 69–85.

Cherubini, U., Luciano, E., Vecchiato, W., 2004. Copula Methods in Finance. John Wiley & Sons.

Coulon, M., Powell, W.B., Sircar, R., 2013. A model for hedging load and price risk in the Texas electricity market. Energy Econ. 40, 976–988.

Creal, D., Koopman, S.J., Lucas, A., 2013. Generalized autoregressive score models with applications. J. Appl. Economet. 28 (5), 777–795.

De Lira Salvatierra, I.A., Patton, A.J., 2013, June. Dynamic Copula Models and High Frequency Data. Economic Research Initiatives at Duke (ERID), Working Paper No. 165, Available at SSRN: http://dx.doi.org/10.2139/ssrn.2284235

Dias, A., Embrechts, P., 2004. Dynamic Copula Models for Multivariate High-Frequency Data in Finance. Warwick Business School, Finance Group, Working Paper.

Diks, C.G.H., Panchenko, V., van Dijk, D.J.C., 2010. Out-of-sample comparison of copula specifications in multivariate density forecasts. J. Econ. Dyn. Control. 34 (9), 1596–1609.

Elberg, C., Hagspiel, S., 2015. Spatial dependencies of wind power and interrelations with spot price dynamics. Eur. J. Oper. Res. 241 (1), 260–272.

Embrechts, P., McNeil, A.J., Straumann, D., 1999. Correlation and dependence in risk management: Properties and pitfalls. In: Dempster, M.A.H. (Ed.), Risk Management: Value at Risk and Beyond. Cambridge University Press., pp. 176–223.

Fermanian, J.-D., Wegkamp, M., 2012. Time dependent copulas. J. Multivar. Anal. 110, 19–29.

Gelabert, L., Labandeira, X., Linares, P., 2011. An ex-post analysis of the effect of renewables and cogeneration on Spanish electricity prices. Energy Econ. 33, 59–65.

Genest, C., Remillard, B., Beaudoin, D., 2009. Goodness-of-fit tests for copulas: A review and a power study. Insur. Math. Econ. 44 (2), 199–213.

Giacomini, R., White, H., 2006. Tests of conditional predictive ability. Econometrica 74 (6), 1545–1578.

González-Pedraz, C., Moreno, M., Peña, I., 2015. Portfolio selection with commodities under conditional copulas and skew preferences. Quant. Finan. 15 (1), 151–170.

Joe, H., 1997. Multivariate Models and Dependence Concepts. 1st Edition, Chapman and Hall. 978-0412073311

Jónnson, T., Pinson, P., Madsen, H., 2010. On the market impact of wind energy forecasts. Energy Econ. 32 (2), 313–320.

Kolos, S.P., Ronn, E.I., 2008. Estimating the commodity market price of risk for energy prices. Energy Econ. 30 (2), 621–641.

Lucia, J.J., Schwartz, E.S., 2000. Electricity prices and power derivatives: Evidence from the Nordic Power Exchange. Rev. Deriv. Res. 5, 5–50.

McKinnon, R.I., 1967. Future markets, buffer stocks, and income stability for primary producers. J. Polit. Econ. 75 (6), 844–861.

Moschini, G., Lapan, H., 1995. The hedging role of options and futures under joint price, basis, and production risk. Int. Econ. Rev. 36 (4), 1025–1049.

Nelsen, R.B., 1999. An Introduction to Copulas. Springer.

Nelson, D.B., Cao, C.Q., 1992. Inequality constraints in the univariate GARCH model. J. Bus. Econ. Stat. 10 (2), 229–235.

Oum, Y., Oren, S.S., 2009. VaR constrained hedging of fixed price load-following obligations in competitive electricity markets. Risk Decis. Anal. 1 (1), 43–56.

Oum, Y., Oren, S.S., 2010. Optimal static hedging of volumetric risk in a competitive wholesale electricity market. Decis. Anal. 7 (1), 107–122.

Oum, Y., Oren, S.S., Deng, S., 2006. Hedging quantity risks with standard power options in a competitive wholesale electricity market. Nav. Res. Logist. 53 (7), 697–712.

Paraschiv, F., Erni, D., Pietsch, R., 2014. The impact of renewable energies on EEX day-ahead electricity prices. Energy Policy 73, 196–210.

Patton, A.J., 2006. Modelling asymmetric exchange rate dependence. Int. Econ. Rev. 47 (2), 527–556.

Patton, A.J., 2013. Copula methods for forecasting multivariate time series. In: Elliott, G., Timmermann, A. (Eds.), Handbook of Economic Forecasting. 2B. Elsevier B.V., pp. 899–960.

Politis, D.N., Romano, J.P., 1994. The stationary bootstrap. J. Am. Stat. Assoc. 89 (428).

Politis, D.N., White, H., 2004. Automatic block-length selection for the dependent bootstrap. Econ. Rev. 23 (1), 53–70.
Politis, D.N., White, H., Patton, A.J., 2009. Correction: Automatic block-length selection for the dependent bootstrap. Econ. Rev. 28 (4), 372–375.
Rivers, D., Vuong, Q., 2002. Model selection tests for nonlinear dynamic models. Econ. J. 5, 1–39.
Schepsmeier, U., Stöber, J., 2014. Derivatives and Fisher information of bivariate copulas. Stat. Pap. 55 (2), 525–542.
Sklar, A., 1959. Fonctions de répartition à n dimensions et leurs marges. Publications de l'Institut de Statistique de L'Université de Paris 8, 229–231.
Wen, X., Wei, Y., Huang, D., 2012. Measuring contagion between energy market and stock market during financial crisis: A copula approach. Energy Econ. 34, 1435–1446.